PLASMA DYNAMICS

XV. PLASMA PHYSICS*

Prof. S. C. Brown
Prof. G. Bekefi
Prof. K. U. Ingard
Prof. D. R. Whitehouse
Dr. J. C. Ingraham
M. L. Andrews
V. Arunasalam
C. D. Buntschuh
J. D. Coccoli
F. X. Crist
J. K. Domen
E. W. Fitzgerald, Jr.
D. L. Flannery
G. A. Garosi
W. H. Glenn, Jr.
E. B. Hooper, Jr.
P. W. Jameson
R. L. Kronquist
J. J. Linehan
D. T. Llewellyn-Jones
J. J. McCarthy
W. J. Mulligan
J. J. Nolan, Jr.
G. L. Rogoff
F. Y-F. Tse
B. L. Wright

RESEARCH OBJECTIVES

The aim of this group continues to be the study of the fundamental properties of plasmas. We have been placing particular emphasis on plasmas in magnetic fields, plasmas of high percentage ionization at low pressures, and most recently on a plasma showing turbulence in high-speed flow.

We are also studying ways of determining the characteristics of plasmas by means of very far infrared optics in the wavelength range 0.1-1 mm, and by means of optical lasers.

The infrared diagnostic techniques are closely correlated with our continued effort to improve the more standard microwave methods. Most of our microwave techniques at the present time involve the study of microwave radiation from plasmas, with and without magnetic fields.

Theoretical work has been concentrated on the study of waves in plasma, turbulence in flowing gases, and the statistical nature of plasmas.

S. C. Brown

A. SCATTERING OF MICROWAVES FROM "COLLECTIVE DENSITY FLUCTUATIONS" IN PLASMAS

The dispersion relation for a plasma of electrons and ions in general has two roots (normal modes). One of these normal modes is the high-frequency optical mode (the electron plasma oscillations) in which the electrons and ions move out of phase, and the other is the low-frequency acoustic mode (the ion plasma oscillations) in which the electrons and ions move in phase. If one produces a plasma in which the electrons have a steady drift velocity with respect to the ions, then the velocity distribution functions take the forms

$$f_{-}(v) = \frac{1}{\sqrt{2\pi}\, v_{-}} \exp\left[-(v-v_d)^2 / 2v_{-}^2 \right] \tag{1a}$$

and

*This work was supported in part by the U.S. Atomic Energy Commission (Contract AT(30-1)-1842); and in part by the U.S. Air Force (Electronic Systems Division) under Contract AF19(604)-5992.

$$f_+(v) = \frac{1}{\sqrt{2\pi}\, v_+} \exp\left[-v^2/2v_+^2\right]. \tag{1b}$$

Here, for the electrons and ions,

$$v_\mp^2 = \frac{KT_\mp}{m_\mp}.$$

It is clear from expression (1a) that $f_-(v)$ increases as v increases for electron velocities $v \leq v_d$. If this drift velocity is large enough for the phase velocity of any one of the normal modes mentioned above to satisfy the inequality $v_p = \frac{\omega}{k} \leq v_d$, then it is possible for the waves of that normal mode to grow in amplitude.

Such a growth in the amplitude of the wave is a consequence of the transfer of the "extra" kinetic energy of those electrons whose velocities lie in the neighborhood of the phase velocity of the wave to that wave under consideration. If, furthermore, the wave frequency is sufficiently large compared with the frequency appropriate to the damping mechanism (that is, the collision frequency), then it can be shown that the growth rate of these waves can exceed unity. Thus for sufficiently large drift velocities and sufficiently low collision frequencies, it is possible to have plasma wave instabilities. It can be shown that the density-density correlation function corresponding to the "collective density fluctuations" exhibits a huge increase as the plasma from a region of stability approaches a critical point corresponding to the onset of the above-mentioned plasma wave instabilities. Consideration of the theory of electromagnetic wave scattering leads us to predict enormously increased scattering of the electromagnetic radiation from such "collective density fluctuations." In such a scattering the difference between the frequency of the scattered radiation and the frequency of the incident radiation is equal to the frequency of the wave responsible for the scattering, and the scattering cross section is approximately proportional to the potential energy of the wave responsible for the scattering.

Once the instability sets in, the amplitude of the "plasma oscillations" presumably becomes sufficiently large that nonlinear effects such as the coupling between plasma modes of different wavelengths begin to play a role. This coupling will cause the modes of lower wave numbers to decay into modes of a higher wave number. The higher wave-number modes decay, in turn, into still higher wave-number oscillations, until presumably those oscillations whose wave number is approximately equal to the reciprocal of the Debye length decay into fine-grained random or thermal motion. Since these oscillations grow by absorbing the necessary energy from the directed particle motion, we conclude that the relative drift velocity will tend to saturate near the threshold for creation of those high wave-number unstable oscillations that are capable of decaying directly into a fine-grained random or thermal motion.

Ichimaru,[1] Ichimaru, Pines, and Rostoker,[2] and Pines and Schrieffer[3] have analyzed the theory of the plasma wave instabilities in detail. They point out that the scattering of electromagnetic waves by electron density fluctuations in a plasma is determined by $S(\vec{k},\omega)$, the Fourier transform of the electron density-density correlation function. The differential cross section, $d^2\sigma/d\Omega\, d\omega$, for the transfer of momentum $\hbar k$ (for scattering into a solid angle $d\Omega$) and energy $h\omega$ from an electromagnetic wave to the electrons in a plasma is given by

$$\frac{d^2\sigma}{d\Omega d\omega} = \left(\frac{e^2}{m_- c^2}\right)^2 \left(1 - \frac{1}{2}\sin^2\theta\right) S(\vec{k},\omega), \tag{2}$$

where θ is the angle between the incident and scattered waves. $S(\vec{k},\omega)$ is defined as

$$S(\vec{k},\omega) = \frac{L^3}{2\pi} \int_{L^3} d\vec{r} \int_{-\infty}^{\infty} dt \left\langle n(\vec{r}'+\vec{r}, t'+t) n(\vec{r}', t') \right\rangle e^{-i(\vec{k}\cdot\vec{r} - \omega t)}, \tag{3}$$

where N is the total number of electrons in a volume L^3, $n(\vec{r},t)$ denotes the electron number density, and the angular brackets refer to a statistical average over the electron states. The measurement of the intensity of radiation scattered into a given angle yields directly the structure factor $S(\vec{k})$, which is

$$S(\vec{k}) = \frac{1}{N} \int_{-\infty}^{\infty} d\omega\, S(\vec{k},\omega). \tag{4}$$

By using the distribution functions given by Eqs. 1 in the Boltzmann-Poisson equations, Ichimaru and others[1-3] derived an expression for the longitudinal dielectric coefficient $\epsilon(\vec{k},\omega)$. By letting Im $\epsilon[\vec{k},\omega(\vec{k})] = 0$, they obtained the boundary between the growing and damped ion acoustic waves. They represent this boundary by a curve $\vec{v}_d(\vec{k})$ in the $\vec{v}_d$-$\vec{k}$ plane, and the equation of this boundary is given by

$$v_d(k) = v_{d_1}(k) + v_{d_2}(k). \tag{5}$$

Here,

$$\frac{v_{d_1}(k)}{v_-} = \frac{(m_-/m_+)^{1/2}}{[1+(k^2/k_-^2)]^{1/2}} \left\{ 1 + \left(\frac{m_+}{m_-}\right)^{1/2} \left(\frac{T_-}{T_+}\right)^{3/2} \exp\left[-\frac{1}{2}\left(\frac{T_-/T_+}{1 + k^2/k_-^2} + 3 \right) \right] \right\} \tag{6}$$

and

$$\frac{v_{d_2}(k)}{v_-} = \sqrt{\frac{2}{\pi}} \frac{1}{\omega_+ \tau_+} \frac{[1+k^2/k_-^2]^{3/2}}{k/k_-}, \tag{7}$$

where τ_+ is the relaxation time of the ions, $\omega_+ = 2\pi f_+ = (4\pi n_+ e^2/m_+)^{1/2}$, and $k_- = (4\pi n_- e^2/KT_-)^{1/2}$. Letting Re $\epsilon[\vec{k},\omega(\vec{k})] = 0$, we obtain the dispersion relation for the ion acoustic plasma oscillations:

$$\frac{f}{f_+} = \frac{\omega}{\omega_+} = \frac{k/k_-}{[1+k^2/k_-^2]^{1/2}}. \tag{8}$$

This equation can be rewritten in a convenient form

$$\frac{k_-^2}{k^2} = \left[\frac{f_+^2}{f^2} - 1\right]. \tag{9}$$

From Eqs. 5-7 we can define a critical point k_c as that wave vector for which, with increasing drift velocity $\vec{v}_d$, the ion sound wave first becomes unstable. Let $v_c = v_d(k_c)$ be the associated minimum drift velocity for instability. Using such a notation, they show that just at the onset of the ion acoustic plasma wave instability the dynamic form factor $S(\vec{k},\omega)$ and the structure factor $S(\vec{k})$ are given by

$$S_{crit}(\vec{k},\omega) = \frac{N}{\sqrt{2\pi}\, kv_-}\left[\frac{1}{\left\{1-[\omega(k)^2/\omega^2]\right\}^2 + \pi\left\{[(v_c-v_d)+v_1(k^2/k_-^2)]/v_-\right\}^2/2}\right]^{1/2} \tag{10}$$

$$S_{crit}(\vec{k}) = \frac{1}{2}\left|\frac{(m_-/m_+)^{1/2}}{\{[v_c-v_d]/v_- + (v_1/v_-)(k^2/k_-^2)\}}\right| \tag{11}$$

for $k^2 < k_-^2$ and $k_c = 0$.

For sufficiently large temperature ratios (say, $T_-/T_+ > 10$),

$$\frac{v_1}{v_-} \approx \frac{1}{2}\left\{\left[\left(\frac{T_-}{T_+}\right)^{5/2} e^{-[(T_-/T_+)+3]/2}\right] - \left(\frac{m_-}{m_+}\right)^{1/2}\right\}. \tag{12}$$

Using Eqs. 5-7 we have plotted Fig. XV-1 for a hydrogen plasma. Here $(m_-/m_+)^{1/2} \approx 1/43$. For $(T_-/T_+) \approx 25$ and $500 \leq \omega_+\tau_+ \leq 1000$ we see from Fig. XV-1 that $k_c \approx 0$, and $v_c = v_d$ for "marginal stability," and $(v_1/v_-) \approx -\frac{1}{2}(m_-/m_+)^{1/2}$. Under these conditions, $S_{crit}(\vec{k})$ of Eq. 11 reduces to the approximate form

$$S_{crit}(\vec{k}) \approx \frac{1}{(k^2/k_-^2)} = \frac{k_-^2}{k^2}. \tag{13}$$

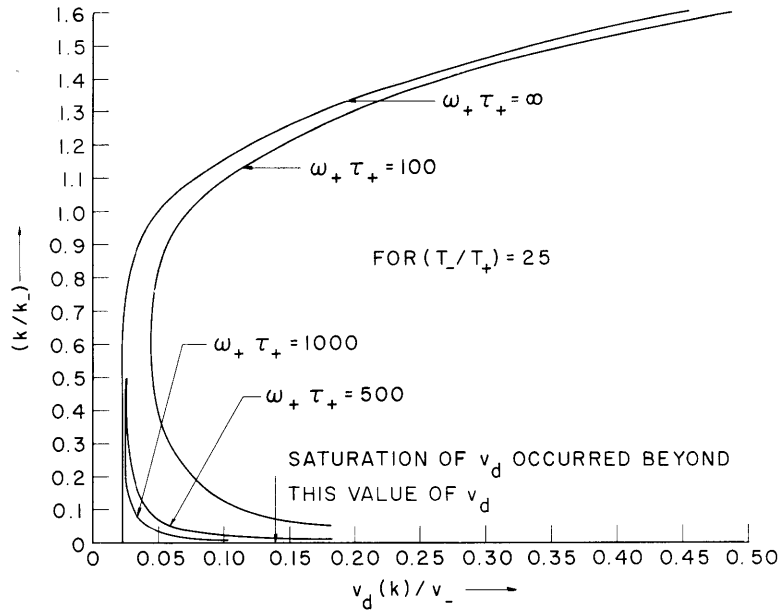

Fig. XV-1. Boundary between growing and damped waves as a function of drift velocity.

Using Eq. 9, we can go from momentum space to energy space, and, by using Eq. 13, we can define the structure factor in energy space appropriate to the critical condition:

$$S_c(f) = [(f_+^2/f^2)-1]. \tag{14}$$

If we measure the intensity of the scattered radiation collected over all angles $\theta \gg \theta_o$ around the critical angle θ_c as a function of frequency f, then, with the aid of Eq. 2, we are led to relate the total cross section $\sigma_c(f)$ to the Thomson cross section $\sigma_o = \frac{8\pi}{3}(e^2/m_-c^2)^2$ as

$$\sigma_c(f) = \sigma_o S_c(f) = \sigma_o[(f_+^2/f^2)-1] \tag{15}$$

and

$$\sigma_c(f) = \int_{-B/2}^{B/2} \left(\frac{d\sigma}{df}\right)_c df,$$

where B is the bandwidth of the detector instrument, and

$$\theta_c = 2 \sin^{-1}(k_c/2k_i)$$
$$\theta_o = 2 \sin^{-1}(k_-/2k_i). \tag{16}$$

Here, k_i is the wave number that the incident radiation will have inside the plasma, and this is related to the wave number k_o of the incident radiation in free space by the

relation $k_i = k_o \, \mathrm{Re}\,[\epsilon^{1/2}]$, where ϵ is the dielectric coefficient of the plasma appropriate to the incident radiation. If the plasma is in a magnetic field, ϵ will depend on the directions of $\vec{E}$ and $\vec{k}_o$ with respect to the magnetic field.[4] Furthermore, it is quite likely that condition (16) need not be satisfied in the presence of a uniform magnetic field $\vec{B}$, since the vector potential for such a $\vec{B}$ field may be written as $\vec{A} = \frac{1}{2}\vec{B} \times \vec{r} + \vec{\nabla} f(r)$, where f(r) is any arbitrary function of the coordinate. This arbitrariness in $\vec{A}$ generally allows us to ignore the momentum conservation relations, since the canonical momenta of electrons and ions responsible for the wave are also arbitrary to some extent when a magnetic field is present.

The scattered power is given by

$$P_s(f) = n_- \sigma_c(f) \,(\text{volume of scatterer}) \left(\frac{\text{incident power}}{\text{area}}\right). \tag{17}$$

It is interesting to note from Eqs. 15 and 17 that for $f^2 \ll f_+^2$

$$\sigma_c(f) \sim \frac{n}{f^2} \tag{18}$$

and

$$P_s(f) \sim \frac{n^2}{f^2}, \tag{19}$$

in which we have used the reasonable assumption that $n_- \approx n_+ \approx n$ (say).

The discharge current is generally given by

$$(J/\text{area}) = j = nev_d. \tag{20}$$

If the drift velocity saturates and the area remains constant, then Eqs. 18-20, for $f^2 \ll f_+^2$, give

$$\sigma_c(f) \sim (J/f^2) \tag{21}$$

and

$$P_s(f) \sim (J^2/f^2). \tag{22}$$

It should be noted that this analysis assumes that the drift velocity is in the direction of $\vec{k}$ of the ion acoustic wave responsible for the scattering.

The experimental arrangement is illustrated in Fig. XV-2. The over-all length of the discharge tube used for the production of the plasma is approximately 15 cm, and the diameter of the Pyrex plasma tube is approximately 2 cm. The distance between the two probes on either side of the scattering volume is approximately 6.5 cm. The cathode is an oxide-coated tungsten spiral. The shield around the cathode is a cylindrical can of

molybdenum. The shield is tied to one of the cathode leads and insulated from the other cathode lead by an insulation bead. The face of the water-cooled anode is of stainless steel and the rest of it is of copper. A magnetic field of 2290 gauss was applied parallel to the axis of the discharge tube with the aid of an electromagnet.

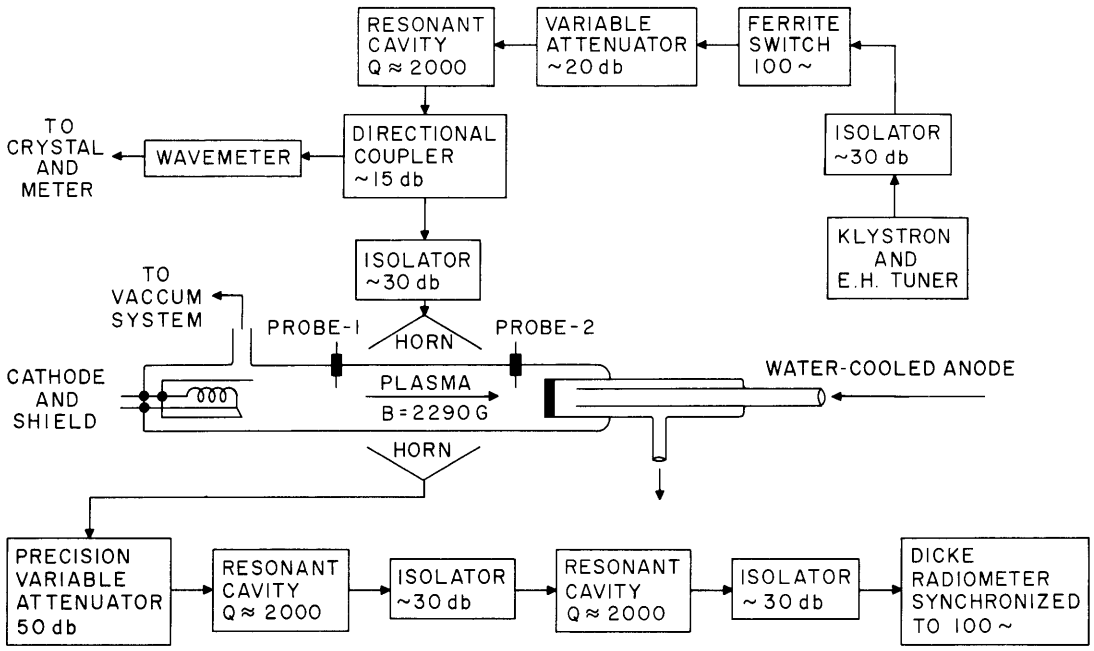

Fig. XV-2. Experimental arrangement.

In the actual experiment the discharge tube was initially evacuated to a pressure of 10^{-7} mm Hg, and hydrogen gas from a litre bottle attached to the vacuum system was admitted into the discharge tube until the pressure was 80 μ Hg as read by the McLeod gauge. The maximum discharge current used for the measurement was 1 amp. Readings were taken for discharge currents in steps of 1/10 amp. The voltage across the two probes was measured for each current. This voltage varied from 19 volts to 25 volts as the discharge current was increased from 0.1 amp to 0.3 amp, but remained relatively constant (within ±2 volts of 26 volts) for the range 0.3-1.0 amp. There were no visible dark spaces in the discharge. In appearance the plasma is of cylindrical shape, with a 4-mm diameter, and extends from cathode to anode.

The incident X-band microwave power was supplied by a Varian X-13 klystron, and the incident frequency was varied from 9140 mc to 9380 mc by steps of approximately 8 mc for the purposes of scanning the scattered spectrum. With the aid of the directional coupler, wavemeter, crystal, and meter in the incident line, the frequency of the incident power was read directly in megacycles, and the incident power was held

constant as the frequency spectrum was scanned. The Dicke radiometer and all of the resonant cavities in the detector line were tuned to a fixed frequency of 9255 mc. The incident power of approximately 90 mw (only 1/36 of this power reaches the plasma because of attenuation of approximately 16 db in the line) was modulated in the line by the ferrite switch at 100 cps, and the radiometer was synchronized to this modulation frequency. With the aid of the three resonant cavities, each of $Q \approx 2000$, we were able to avoid any direct pickup as the incident frequency was brought to approximately 7 mc on each side of the detector frequency. The horns used in the incident and detector lines are X-band to C-band transitions. The $\vec{E}$ and $\vec{k}$ vectors of both the incident and detector lines were kept perpendicular to the uniform magnetic field of 2290 gauss.

The ion density, $n_+ \approx n$, was determined from the ratio (slope/intercept) = f_+^2 of the straight-line graph in Fig. XV-6. The electron density $n_- \approx n$, measured by determining the plasma "cutoff" condition of the extraordinary wave, was found to agree reasonably with this value of the ion density. The drift velocity was then calculated with the aid of Eq. 20. Also, from the knowledge of the measured values of E/p, where p is the pressure, the drive velocity was calculated. The value of the drift velocity as given by Eq. 20 was found to be five times larger than that given by E/p measurements. With the aid of Sanborn C. Brown's data,[5] under the assumption that the ions are approximately ten times hotter than the background gas (that is, $T_+ \approx \frac{1}{4}$ ev), we estimated the values of T_-/T_+, $\tau_+ = 1/\nu_+$, and v_-. The bandwidth of the radiometer was measured by comparing a known fraction of the klystron power with that of a standard noise tube of known radiation temperature: $P = kTB$.

Experimental data are summarized below.

Data and Results

Gas	Hydrogen
Pressure of gas	$\approx 80\ \mu$ Hg
Plasma electric field $\vec{E}$	≈ 4 volts/cm
$\therefore$ E/p	≈ 50 volts/cm-mm Hg
Variation in E/p as current was varied from 0.1 amp to 0.3 amp	≈ 10 volts/cm-mm Hg
Variation in E/p as current was varied from 0.3 amp to 1.0 amp	≈ 4 volts/cm-mm Hg
Diameter of the cylindrical plasma column	≈ 0.4 cm
Scattering length of plasma column	≈ 5 cm
Total length of plasma column	≈ 11 cm

Data and Results (continued)

Magnetic field, $\vec{B}$	2290 gauss
$\therefore$ The electron-cyclotron frequency f_b	6400 mc
The ion plasma frequency f_+ calculated from Fig. XV-6. Here, J is the total discharge current in amperes	$140\sqrt{J}$ mc
$\therefore$ The electron plasma frequency f_-	$\approx 6000\sqrt{J}$ mc
$\therefore$ The electron density $n_- \approx n$	$\approx 4.5 \times 10^{11}$ J/cm^3
For incident frequency of 9200 mc, the plasma cutoff condition for extraordinary wave occurred at	≈ 0.9 amp
For the electron plasma frequency f_- this gives	$\approx 5400\sqrt{J}$ mc
Drift velocity calculated by using n_- and Eq. 20	$\approx 1.1 \times 10^8$ cm/sec
Drift velocity calculated by using E/p and Fig. 3.2 of S. C. Brown[5]	$\approx 2 \times 10^7$ cm/sec
Electron temperature T_- calculated by using E/p and Fig. 3.53 of S. C. Brown[5]	≈ 6 volts
$\therefore\ v_- = \left(\frac{KT_-}{m_-}\right)^{1/2}$	$\approx 1.45 \times 10^8$ cm/sec
The value of (v_d/v_-) was in the range	$0.14 \lesssim (v_d/v_-) \lesssim 0.76$
(T_-/T_+), by assuming $T_+ \approx \frac{1}{4}$ volt	≈ 24
$\nu_+ = \frac{1}{\tau_+}$ for $T_+ \approx \frac{1}{4}$ volt by using Fig. 1.50 of S. C. Brown[5]	≈ 1.2 mc
$\therefore\ \omega_+\tau_+ = 2\pi f_+\tau_+$	$\approx 730\sqrt{J}$
Power sent out by klystron ($\approx$16 db loss on line)	≈ 90 mw
Incident power for scattering	≈ 2.5 mw
Measured bandwidth B of radiometer	≈ 0.75 mc

In Fig. XV-3 we have plotted the scattering cross section $\sigma_c(f)$ as a function of (f/f_+) as given by the theoretical equation (15), and in the same figure we have shown the experimental measurements of $\sigma_c(f)$, in which the point corresponding to $\sigma_c(f) = 400\,\sigma_o$ was fitted to the theoretical curve. In plotting the data taken at currents of 0.3, 0.4,

0.5, 0.6, 0.7, 0.8, 0.9, and 1.0 amp, we have made use of Eq. 21 and the relation that $f_+ \sim \sqrt{J}$. This graph seems to confirm the correctness of Eqs. 15 and 21. In Fig. XV-4

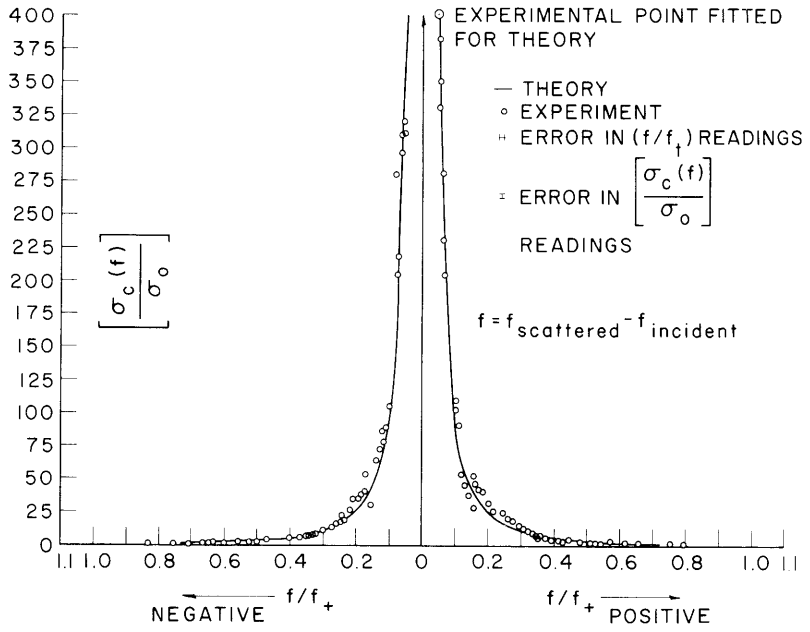

Fig. XV-3. Scattering cross section $\sigma_c(f)$ as a function of wave frequency f.

we have plotted the scattered power as a function of the square of the discharge current for given frequency difference between the incident and scattered frequencies. In Fig. XV-4a, the frequency of the scattered radiation is less than that of the incident radiation, and in Fig. XV-4b, the scattered radiation is of higher frequency than the incident radiation. In Fig. XV-5, we have plotted the slopes of the straight-line graphs of Fig. XV-4 as a function of $1/f^2$, where f is the difference between the incident and scattered frequencies. These graphs in Figs. XV-4 and XV-5 seem to confirm the correctness of Eq. 22 reasonably well.

In Fig. XV-6 we have plotted the scattered power as a function of $1/f^2$ for a discharge current of 1.0 amp. Using the relation

$$f_+^2 = \left(\frac{n_+ e^2}{\pi m_+}\right) = \left(\frac{\text{slope}}{\text{intercept on } P_s \text{ axis}}\right)$$

for the straight-line graph in Fig. XV-6, we calculated the ion plasma frequency f_+ and the ion density $n_+ \approx n$.

From Eqs. 15, 17, and 20 one can show that for $f^2 < f_+^2$

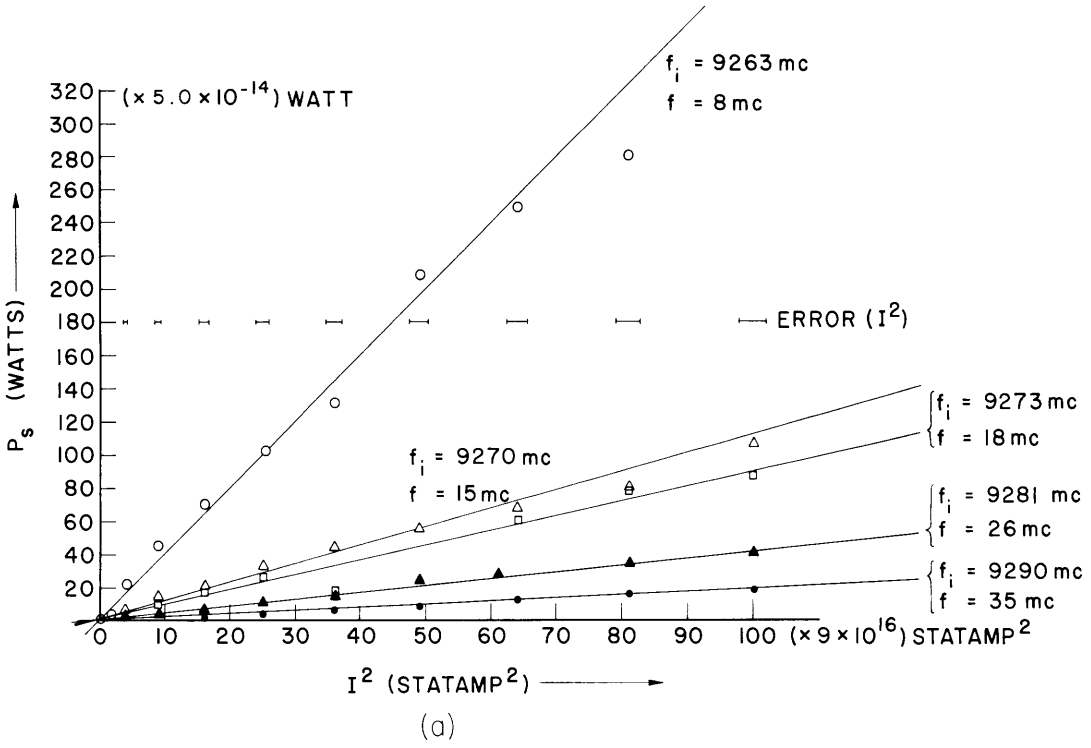

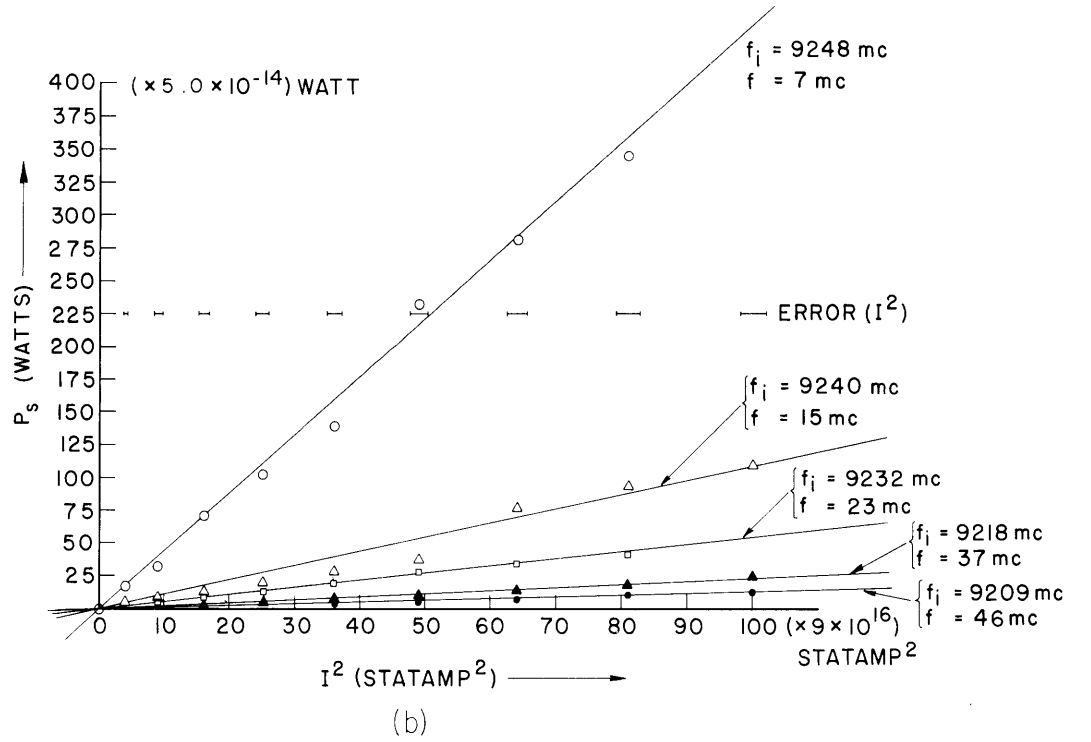

Fig. XV-4. Scattered power vs square of the discharge current J. (a) Scattered frequency less than incident frequency. (b) Scattered frequency greater than incident frequency.

$$P_s(f) = \left[\frac{4\sigma_o(\text{incident power})}{\pi^2 m_+ d^3 v_d^2}\right]\left(\frac{J^2}{f^2}\right), \tag{23}$$

where d is the diameter of the cylindrical plasma column. Using Eq. 23 and the slope of the graph in Fig. XV-5, we get

$$\sigma_o \approx \begin{cases} 5.90 \times 10^{-24}\ \text{cm}^2 & \text{if } v_d \approx 2 \times 10^7\ \text{cm/sec} \\ 1.79 \times 10^{-22}\ \text{cm}^2 & \text{if } v_d \approx 1.1 \times 10^8\ \text{cm/sec.} \end{cases}$$

But the actual value of the Thomson cross section $\sigma_o = \frac{8\pi}{3}(e^2/m_e c^2)^2 \approx 6.6 \times 10^{-25}\ \text{cm}^2$.

This analysis of the experimental results seems to indicate that the measured scattering cross section $\sigma_m(f)$ satisfies the relation

$$\sigma_m(f) = \delta\sigma_c(f) = \delta\sigma_o\left[\frac{f_+^2}{f^2} - 1\right], \tag{24}$$

where the enhancement factor δ is not a function of f or f_+. Comparing Eq. 24 with the theoretically calculated equation (15) for "marginal stability," we see that this enhancement factor δ is a measure of the level of the ion plasma oscillations which exists at steady state with respect to that at the "marginal stability." Therefore this enhancement factor δ is a measure of the nonlinear coupling between the plasma modes

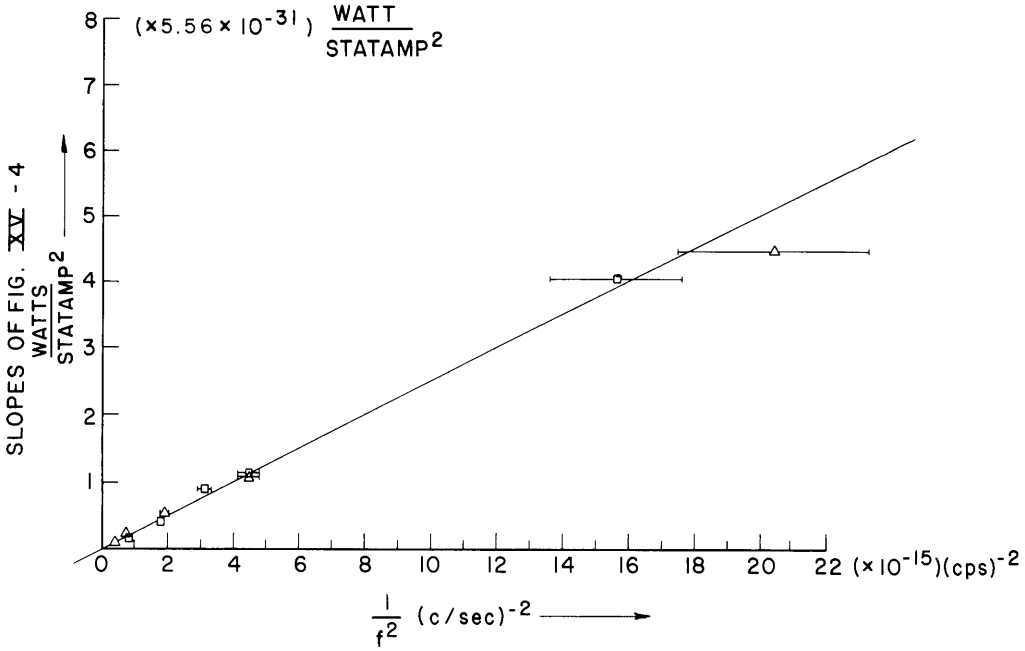

Fig. XV-5. Slopes of Fig. XV-4a and 4b versus $1/f^2$.

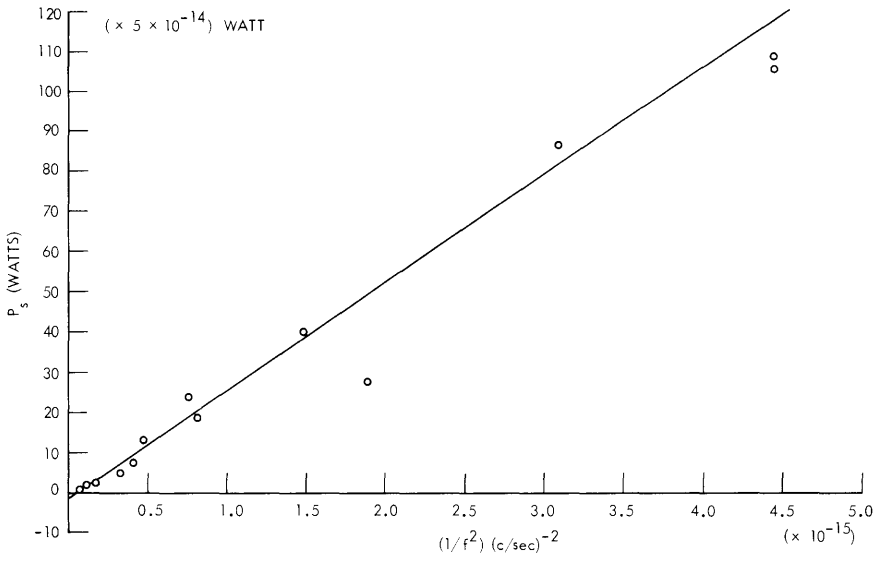

Fig. XV-6. Scattered power versus $1/f^2$ for 1.0-amp discharge current.

of different wavelengths. For a given value of the relative drift velocity $v_d \gtrsim v_c$, the weaker are the nonlinear effects, the larger is the portion of the available drift energy going into the plasma oscillations. Thus if the nonlinear effects are very weak, one will expect this enhancement factor δ to be very much larger than unity, since the plasma will reach a steady state far beyond the conditions of "marginal stability," and if the nonlinear effects are very strong δ will be equal to unity, since the plasma will reach a steady state almost at the conditions of "marginal stability." Our experimental results yield

$$\delta \approx \begin{cases} 9.0 & \text{if } v_d \approx 2 \times 10^7 \text{ cm/sec} \\ 270 & \text{if } v_d \approx 1.1 \times 10^8 \text{ cm/sec.} \end{cases}$$

Thus the experimental measurement of δ seems to indicate that the nonlinear coupling between the plasma modes of different wavelengths is not too strong.

The results presented in Figs. XV-3, XV-4, and XV-5 seem to be in reasonable agreement with the theory of Ichimaru,[1] and Ichimaru, Pines, and Rostoker.[2] The experimental verification of Eq. 22, along with the observed approximate constancy of the value of E/p as the discharge current was varied from 0.3 amp to 1.0 amp, seems to indicate that the drift velocity tends to saturate. From the measured value of this saturation drift velocity and Fig. XV-1, we are led to conclude that the saturation of drift velocity occurs near the threshold for the creation of unstable oscillations of wave numbers $k \approx 1.2k_{\_}$. This seems to be reasonable in the light of the qualitative arguments presented by Pines and Schrieffer.[3]

In conclusion, we wish to point out that Newcomb[6] has shown that in the presence of a magnetic field Eq. 8 takes the form

$$\frac{\omega^2}{\omega_+^2} \approx \frac{k^2/k_-^2}{1 + k^2/k_-^2} + \frac{\Omega^2 \sin^2 \alpha}{\omega_+^2},$$

where $\Omega = (eB/m_+ c)$ is the ion-cyclotron frequency and α is the angle between $\vec{k}$ and $\vec{B}$. For regions of interest to us here $\Omega^2/\omega_+^2 \ll k^2/k_-^2$, and therefore the correction term to Eq. 8 is negligible. Furthermore, in our experiment $\alpha \approx 0$, and thus the correction term to Eq. 8 is approximately zero.

V. Arunasalam

References

1. S. Ichimaru, Ann. Phys. 20, 78-118 (1962).

2. S. Ichimaru, D. Pines, and N. Rostoker, Phys. Rev. Letters 8, 231 (1962).

3. D. Pines and J. R. Schrieffer, Phys. Rev. 124, 1387-1400 (1961).

4. W. P. Allis, S. J. Buchsbaum, and A. Bers, Waves in Anisotropic Plasmas (The M.I.T. Press, Cambridge, Mass., 1963).

5. S. C. Brown, Basic Data of Plasma Physics (The Technology Press of the Massachusetts Institute of Technology, Cambridge, Mass., and John Wiley and Sons, Inc., New York, 1959).

6. W. A. Newcomb, Ion Oscillations in a Magnetic Field, Report UCRL-4941, Livermore, California, July 30, 1957.

B. SCATTERING FROM PLASMA OSCILLATIONS IN THE PRESENCE OF AN INHOMOGENEOUS MAGNETIC FIELD

Electromagnetic radiation has been scattered from a plasma in an inhomogeneous magnetic field. Under those plasma conditions for which the plasma contains strong oscillations, a large enhancement of the scattering cross section has been found as a result of the presence of the inhomogeneous field. When an electromagnetic wave is scattered from a plasma, the scattered frequencies correspond to the sum and differences of the incident frequency and the frequencies of the plasma oscillations. In the presence of an inhomogeneous field the dispersion relation can contain resonances both at the incident and at the scattered frequencies, thereby giving rise to a large increase in the scattering cross section.

1. Plasma and Plasma Oscillations

The plasma used in the experiment was a cesium hot cathode discharge.[1] The pressure of the cesium was 0.1-5 μ Hg and was controlled by the temperature of the

discharge tube. The discharge was approximately 1 meter long, and the cathode was an oxide-coated ribbon. The phenomena of interest occurred for discharge currents of a few milliamperes, or electron densities of approximately $10^8/cm^3$, and for external magnetic fields of approximately 1000 gauss.

The plasma had three different modes of operation. The first mode was one in which the plasma was electrically very quiet. This mode existed only for low cesium pressures ($\lesssim 0.2$ μ Hg), and for low discharge currents ($\lesssim 2$ ma). The voltage across the meter-long discharge tube was typically 10 volts in this mode of operation.

The second mode of operation was most easily observed as a transition from the first mode as the discharge current was raised. Strong oscillations appeared in the current, and the voltage across the discharge tube jumped to over 400 volts. The frequency of the oscillations (~15 kc) and the values of the critical electric and magnetic fields causing the transition suggest that the second mode was a rotational instability,[2,3] with a wavelength twice the length of the discharge tube. This mode did not exist for pressures above 0.15 μ.

The third mode similarly occurred as a transition from the second, although at cesium pressures above approximately 0.2 μ Hg it was the only mode that was observed. If the current through the discharge was increased while the discharge was in the second mode, the voltage across the discharge abruptly dropped to 14-20 volts. The discharge current in this mode was characterized by strong oscillations in the 10-50 kc frequency range. Although there is no concrete evidence to verify the nature of these oscillations, their frequencies fall in the range of ion acoustic waves.[4]

Also, oscillations in the frequency range 10-100 mc were observed in mode 3 with the aid of a spectrum analyzer. These are the oscillations from which the scattering occurred (see section 3). Because of the frequencies involved, it seems likely that these oscillations were electron oscillations.

2. Emission and Absorption of the Plasma

The interaction of radiation with the plasma was studied by radiometer techniques such as that illustrated in Fig. XV-7. The frequencies used were between 2500 mc and 3100 mc. The plasma was immersed in the magnetic field formed by coils spaced 6 inches apart. This spacing caused a ripple of approximately 3 per cent in the magnetic field.

The cyclotron emission of the plasma is shown in Fig. XV-8. The line shape and line width were caused by the inhomogeneities in the magnetic field. At the pressures used, the collision broadening was estimated to be less than one-tenth of the inhomogeneity broadening.

Absorption measurements were made, and line shapes similar to the emission shape were obtained. The transmission of the plasma was also measured as a function of the DC conductivity of the plasma, and is illustrated for the mode 1 and mode 3 operations

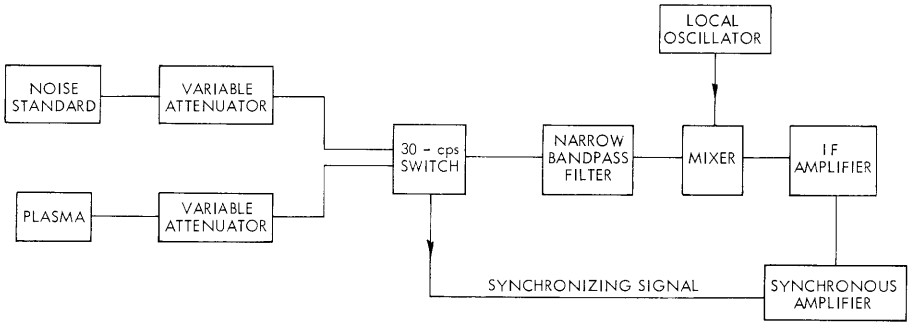

Fig. XV-7. Microwave bridge to measure plasma radiation. Bandwidth of the system, 2 mc. Similar bridge arrangements were used to measure absorption and scattering by the plasma. Plasma was a 1-inch positive column passed through an S-band waveguide at 6°.

(Fig. XV-9). The absorption of the plasma while in mode 2 operation was very small, as would be expected.

As may be seen in Fig. XV-9, absorption was proportional to the current in both mode 1 and mode 3 operation, thereby indicating that the electron density was proportional to the current. The change in slope of the curves for the two cases, however,

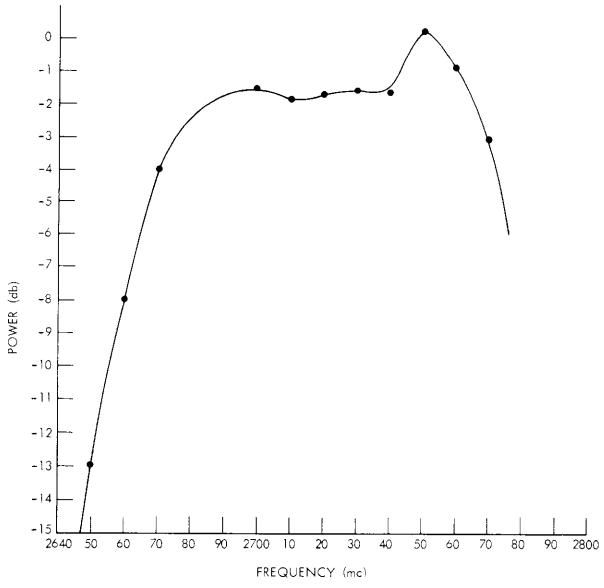

Fig. XV-8. Cyclotron emission from plasma. At 0 db the electron temperature is 10^4°K. Magnet current, 31.35 amps.

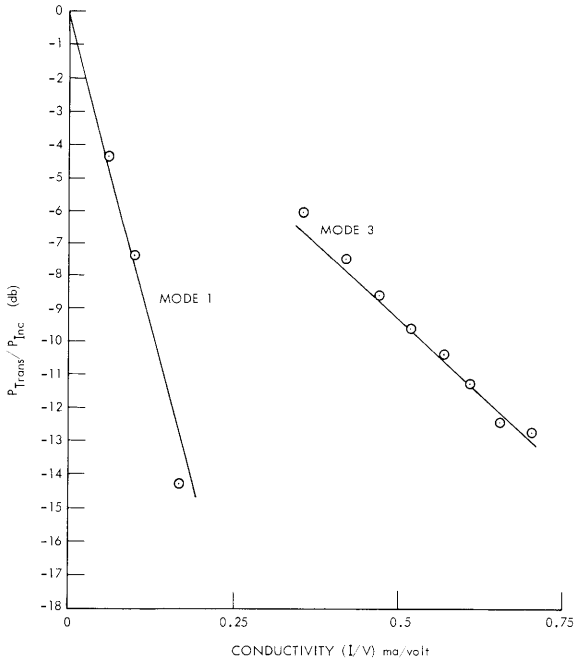

Fig. XV-9. Transmitted power. Cesium pressure, 0.18 μ Hg; frequency, 2705 mc; magnet current, 31.35 amps.

suggests that the electron diffusion mechanism in the plasma changes. This is as expected, for there were strong oscillations in the third mode, which should lead to an enhanced diffusion, although not of the magnitude of that encountered in mode 2.

3. Electromagnetic Scattering

If a signal with a frequency within the cyclotron line was passed through the plasma, there was a strong scattering of radiation. The scattering occurred in all frequencies within the broad resonance, and occurred for all incident frequencies within the resonance (Fig. XV-10). The total scattered energy was approximately one part in 10^6 of

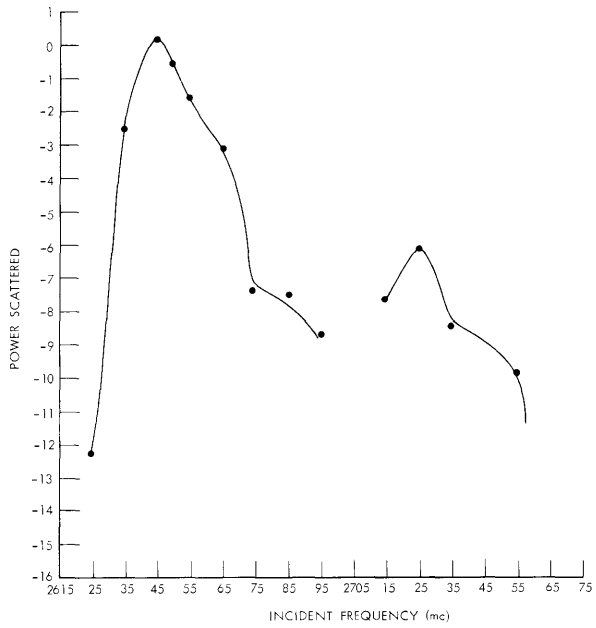

Fig. XV-10.
Scattered power. Measuring frequency, 2705 mc; magnet current, 31.35 amps.

the incident energy.

It can be seen easily that the plasma should resonate both for radiation within the cyclotron line and for scattering within the line. Consider an incident electric field with frequency ω_{inc}. Then, if there are density oscillations in the plasma the Boltzmann equation may easily be solved in the cold-plasma approximation for scattering into a frequency ω. Substituting this solution in the wave equation, for radiation in a waveguide of width a, one finds

$$\frac{d^2E_x}{dz^2}+\left[-\left(\frac{\pi}{a}\right)^2+\frac{\omega^2}{c^2}-\frac{\omega_p^2}{c^2}\frac{(1+i\nu_c/\omega)}{\left(1+\frac{i\nu_c}{\omega}\right)^2-\frac{\omega_B^2(z)}{\omega^2}}\right]E_x=\frac{1}{c^2}\frac{(1+i\nu_c/\omega)}{\left(1+\frac{i\nu_c}{\omega}\right)^2-\frac{\omega_B^2(z)}{\omega^2}}E_x^1(z,\omega_{inc})\,\omega_p^2(z,\omega-\omega_{inc}). \qquad (1)$$

Here, $\omega_p^2(z,\omega-\omega_{inc})$ is the "plasma frequency" corresponding to the oscillating density, and $\omega_B(z) = \frac{eB_z(z)}{m}$. The density is assumed to be uniform across the waveguide, and the radial magnetic field is neglected. With these approximations the scattering term contains the same resonance as the dispersion relation.

If the collision frequency is small enough, the resonance on the right-hand side will "pick out" the oscillations at those values of z for which

$$\omega_B^2(z) = \omega^2 - \nu_c^2. \tag{2}$$

Thus, if there is one resonance, the scattered field will be a measure of the oscillations at one point within the plasma; if there are two resonances, at two points, and hence the two-point correlation function is measured. If there are more resonant points, higher order correlation functions can be measured.

The precise calculation of the scattering requires the solution of Eq. 1, with the proper boundary conditions. The magnetic-field configuration for the scattering discussed earlier is too complicated to find an analytic solution; thus a detailed comparison of the experiment and theory has not been attempted. An approximate solution to the equation for the case of a linear variation in magnetic field has been obtained, however,

$$\frac{E_s(\omega_s)}{E_o(\omega_s)} = \frac{\pi i}{2c^2}\left|\frac{z_s\omega_s}{\omega_B^1(z_s)}\right|\omega_p^2(z_o,\omega_s-\omega_i)\left\{\frac{z_s - z_i - i\nu_c/\omega_B^1(z_i)}{-z_i - i\nu_c/\omega_B^1(z_i)}\right\}e^{i(k_i-k_s)z_o}$$

$$\times F\left(\frac{i\omega_p^2}{4k\omega_B^1(z_s)\,\omega_s}\,|\,1\,|2ik\left(L - z_s - \frac{i\nu_c}{\omega_B^1(z_s)}\right)\right)\frac{F\left(\frac{i\omega_p^2}{4k\omega_B^1(z_i)\,\omega_s}\,|\,1\,|2ik\left(z_o - z_1 - \frac{i\nu_c}{\omega_B^1(z_i)}\right)\right)}{F\left(\frac{i\omega_p^2}{4k\omega_B^1(z_i)\,\omega_s}\,|\,1\,|-2ik\left(z_1 + \frac{i\nu_c}{\omega_B^1(z_i)}\right)\right)} \tag{3}$$

In this equation E_s is the field scattered at a frequency ω_s, and E_o is the transmitted field, if a field of the same amplitude as the incident field, but with frequency ω_s, is passed through the plasma. z_s is the point at which ω_s resonates, and z_i is the point at which the incident frequency, ω_i, resonates. $\omega_B^1(z)$ is the derivative of the cyclotron frequency. k is the wave vector in the absence of a plasma, and thus

$$k_s^2 = \frac{-\pi^2}{a^2} + \frac{\omega_s^2}{c^2} \text{ and } k_i^2 = \frac{-\pi^2}{a^2} + \frac{\omega_i^2}{c^2}.$$

The function F is the confluent-hypergeometric function.[5]

The experimental dependence of the scattered radiation on such parameters as the plasma frequency, the slope of the magnetic field, and so forth, will be compared with Eq. 3 for the case of a single resonance. If the comparison indicates that the approximations used in deriving Eq. 3 are valid, a similar result will be used to determine the correlation function of the oscillations causing the scattering. Study of the low-frequency oscillations, as well as any coupling between these oscillations and the higher frequency oscillations from which the scattering occurs, will be continued.

E. B. Hooper, Jr.

References

1. J. C. Terlouw, Arc discharge in cesium vapor, Quarterly Progress Report No. 63, Research Laboratory of Electronics, M.I.T., October 15, 1961, pp. 5-8.

2. B. B. Kedomsev and A. V. Nedospasov, J. Nuclear Energy 1, Part C, 230 (1960).

3. F. C. Hoh and B. Lehnert, Phys. Rev. Letters 7, 75 (1961).

4. T. H. Stix, The Theory of Plasma Waves (McGraw-Hill Book Company, Inc., New York, 1962), pp. 41-43.

5. P. M. Morse and H. Feshbach, Methods of Theoretical Physics (McGraw-Hill Book Company, Inc., New York, 1953), pp. 550-554, 671-673.

C. ELECTROMAGNETIC COMPRESSION

Attempts are being made to produce a low-pressure plasma by electron-cyclotron resonance breakdown. It is hoped that by using two cavities the electromagnetic compression forces will confine the plasma between the two cavities.

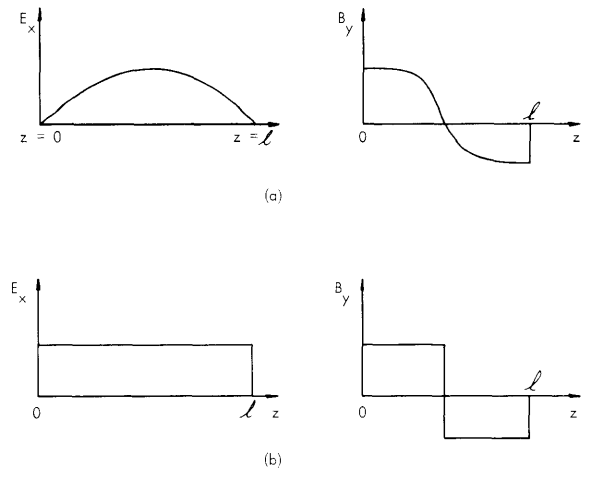

Fig. XV-11.
Electromagnetic fields. (a) Physical fields. (b) Idealized model.

According to the theories of Boot[1] and Hall[2] these forces should approach infinity in the vicinity of cyclotron resonance. From a physical standpoint, we know that this cannot be. Their method utilizes an average over one period of the RF field, whereas it is known that the particle's perpendicular velocity experiences a beat phenomenon of frequency $\omega - \omega_b$. We therefore would like to use a different approach that will be valid in the vicinity of resonance. We also would like to observe the effect of an initial velocity, ignored in previous treatments.

Without a computer it is impossible to perform a calculation of the particles' trajectory inside a cavity. We therefore have made a model of the fields inside the cavity which corresponds roughly to the actual fields but, however, does not satisfy Maxwell's equations. The physical fields are those of a TE_{111}-mode cylindrical cavity. Our field model consists of a uniform electric field in the x-direction with a uniform magnetic field in the y-direction in each half of the cavity. But in each half it has a different sign. (See Fig. XV-11.) Also, we assume another set of fields at right angles to those described above, with a 90° phase shift, so that we have right circular polarization, an assumption that is physically realizable. At present we shall be concerned only with the fields in one-half of the cavity, it being assumed for the present that most of the reflected particles will be reflected before they reach the middle, or not at all. The electric fields in the model can be represented in the following form:

$$
\begin{aligned}
&E_x(t) + jE_y(t) = E\, e^{j\omega t} \\
&B_x(t) + jB_y(t) = -\frac{k}{\omega} E\, e^{j\omega t}, \qquad 0 < z < \frac{\ell}{2},\ k = \frac{\pi}{\ell} \\
&\vec{E}(t) = \vec{B}(t) = 0 \qquad z < 0 \\
&\vec{B}_o = \hat{i}_z B_o.
\end{aligned}
\tag{1}
$$

Defining $w(t) = v_x(t) + jv_y(t)$, we can write the equation of motion of an electron

$$
\frac{d}{dt} w(t) - j\omega_b w(t) = -\frac{e}{m} E\, e^{j\omega t}. \tag{2}
$$

The solution is

$$
w(t) = \frac{-\frac{eE}{m}}{j(\omega - \omega_b)}\left(e^{j\omega t} - e^{j\omega_b t}\right) + v_{\perp o}\, e^{j\omega_b t + j\theta}, \tag{3}
$$

where $v_{\perp o}$ is the perpendicular velocity at $t = 0$.

The z-acceleration can be computed from the Lorentz force.

$$
\frac{dv_z(t)}{dt} = -\frac{e}{m}(\vec{v}\times\vec{B})_z = \frac{e}{m}\,\mathrm{Im}\; w(t)(B_x + jB_y)^*. \tag{4}
$$

Using our solution for w(t), we can integrate this equation to obtain z(t).

$$
\begin{aligned}
z(t) = {} & v_{zo}t - \frac{k}{\omega\delta\omega}\left(\frac{eE}{m}\right)^2 \frac{t^2}{2} - \frac{k}{\omega\delta\omega}\left(\frac{eE}{m}\right)^2 \left(\frac{1 - \cos\delta\omega t}{(\delta\omega)^2}\right) \\
& - \frac{k}{\omega\delta\omega}\frac{eE}{m} v_{\perp o}\left[\cos\theta\left(\frac{\sin\delta\omega t}{\delta\omega} - t\right) + \sin\theta\left(\frac{1 - \cos\delta\omega t}{\delta\omega}\right)\right],
\end{aligned}
\tag{5}
$$

where $\delta\omega = \omega - \omega_b$. The second term on the right-hand side represents the time-averaged force computed by Hall's method; the fourth term is not included in the usual treatments. If $t \gg \frac{1}{\delta\omega}$, Eq. 5 can be approximated by

$$z(t) \approx v_{zo}t - \frac{k}{\omega\delta\omega}\frac{eE}{m}t\left[\frac{eE}{m}\frac{t}{2} - v_{\perp o}\cos\theta\right]. \tag{6}$$

Equation 6 can be solved for the time and place at which the particle stops.

$$z(t_s)\, E\frac{eE}{m\omega}\frac{k}{\delta\omega} = \frac{m}{2e}\left(v_{zo} + \sqrt{\frac{\Omega}{\delta\omega}}v_{\perp o}\cos\theta\right)^2, \tag{7}$$

where

$$\Omega \equiv \frac{k}{\omega}\frac{eE}{m} = \frac{eB_{RF}}{m}. \tag{8}$$

Equation 7 can be represented graphically (see Fig. XV-12). To find the stopping distance, lay off v_{zo} and $\cos\theta\sqrt{\frac{\Omega}{\delta\omega}}v_{\perp o}$, go to the parabola, and read off the ordinate

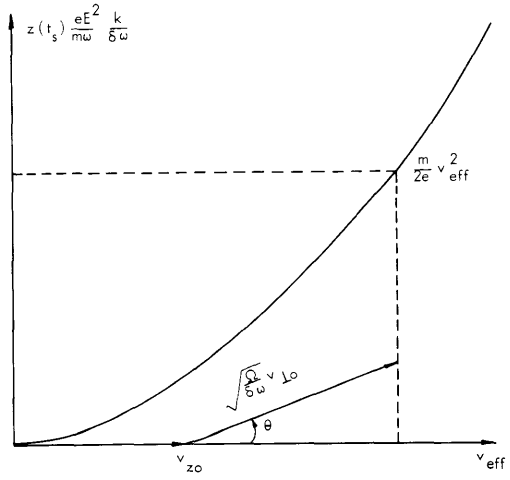

Fig. XV-12. Stopping distance in an applied field, E.

given in normalized stopping distance.

With reference to Eq. 5, we note that if $\delta\omega T \ll \frac{\pi}{2}$ to first order, then there is no time-averaged force because of the forced motion of the particle. This condition corresponds to that for $\omega \approx \omega_b$. It predicts that a large force will be observed only after a very long time and the closer to resonance the longer that time will be.

P. W. Jameson

References

1. H. A. H. Boot, S. A. Self, and R. B. R-Shersby-Harvie, J. Electronics and Control 4, 434-453 (1958).

2. R. B. Hall, Large Signal Behavior of Plasmas, Sc.D. Thesis, Department of Electrical Engineering, M.I.T., September 1960.

D. ANOMALOUS PULSED EMISSION AND ABSORPTION BY A XENON PLASMA AT THE ELECTRON-CYCLOTRON FREQUENCY

Anomalous microwave radiation from xenon, argon, and krypton plasmas in a magnetic field was observed by Tanaka et al.[1] This radiation appeared in the form of a large, very narrow line of radiation at the electron-cyclotron frequency in the pressure range 0.1-5.0 mm Hg. It was suggested by Tanaka et al.[1] that the radiation was a manifestation of the negative radiation temperature predicted by Bekefi, Hirshfield, and Brown[2] and by Twiss.[3]

We have observed several additional features in the emission and absorption of radiation at the cyclotron frequency by a xenon plasma.

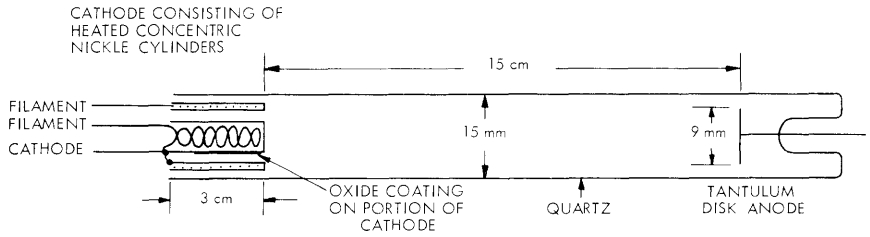

Fig. XV-13. Xenon plasma discharge tube.

The discharge tube is shown in Fig. XV-13. The cathode is similar in construction to the cathode described by Tanaka et al.[1] The anode-to-cathode separation in our discharge tube is 15 cm. The tube diameter is 15 mm. The discharge tube is immersed in the magnetic field of a solenoid. The tube axis coincides with the direction of the magnetic field. The spatial variation in the magnetic field within the volume occupied by the discharge tube is less than 3 gauss per thousand. The measurement was made with a Bell incremental gaussmeter.

The discharge tube passes through the narrow side of a section of S-band waveguide. The microwave electric vector, the direction of propagation, and the external magnetic field are mutually perpendicular.

The pressure of the xenon gas in the discharge tube was measured with a mercury MeLeod gauge. A cold trap filled with Dry Ice and acetone was located between the discharge tube and the McLeod gauge to eliminate mercury vapor from the discharge.

The plasma emission was measured with an S-band radiometer operating synchronously at a 30-cps modulation frequency. The radiometer operated at a fixed frequency

of $\omega/2\pi$ = 3262 mc. The bandwidth of the radiometer IF amplifier was 2 mc. Precision attenuators were used to balance the radiation in the plasma arm against that from an argon noise standard with a radiation temperature of 10,600°K.

The absorption coefficient of the plasma was inferred by measuring the power transmitted through the plasma from an external source. At very low power levels, comparable with the plasma emission level, measurements were performed with the radiometer. The power from the external source was modulated at the synchronous frequency of 30 cps. The plasma emission was not modulated and therefore did not contribute. At high power levels (milliwatts) the radiation was detected by a crystal detector and displayed on an X-Y recorder as a function of the magnetic field. At intermediate power levels (10^{-11}-10^{-8} watt) the signal-to-noise ratio was good enough that the output of the radiometer IF amplifiers could be used without synchronous detection.

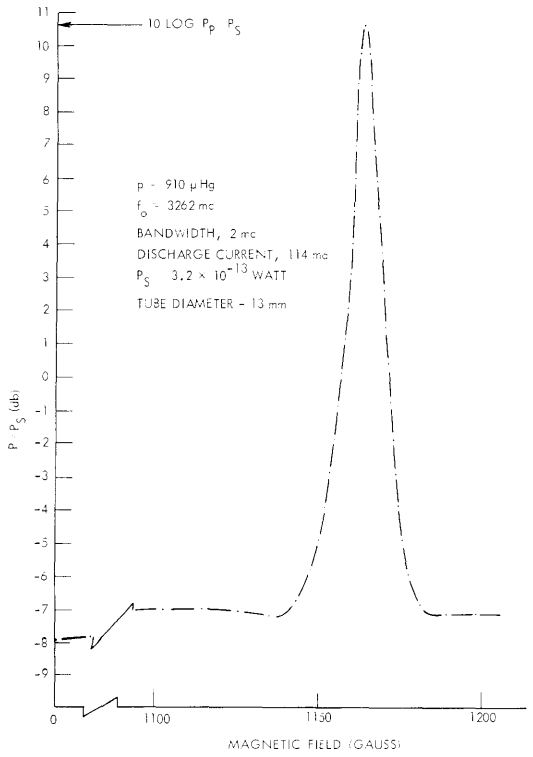

Fig. XV-14. Radiometer measurements of the anomalous cyclotron radiation of a xenon plasma as a function of magnetic field at a fixed microwave frequency.

Figure XV-14 is a typical set of emission data. The ratio of the power radiated from the plasma to that radiated by the noise standard, P/P_S, is presented as a function of the magnetic field at constant discharge current I_d, and constant pressure p. The radiation confirms the features reported by Tanaka et al.[1] It is very narrow, approaching the lower limit imposed by the nonuniformity of the magnetic field. In Fig. XV-14 the amplitude is 17 db above the normal plasma radiation and 11 db above the noise source. This is not as intense as that reported by Tanaka et al.[1] We observed that the amplitude was very sensitive to the orientation of the discharge tube in the magnetic field. In some cases we observed amplitudes 30 db above the normal plasma radiation. Nor did this appear to be a maximum, but further flexing of the glass discharge tube attached to the glass vacuum system seemed unadvisable. Most of the measurements that we shall report were taken with the discharge tube in an in unstrained position. It appears that the position of the cathode surface is important in

determining the nature of the nonthermal distribution of electrons near the cathode. The radiation from a xenon discharge containing a flat cathode surface oriented normal to the external magnetic field did not display the narrow-line radiation. When the tube was turned through a small angle the narrow-line cyclotron radiation was detected, although it was small in amplitude. Thus, it appears important that the electrons near the cathode should be subjected to an acceleration at right angles to the magnetic field.

The amplitude of the narrow-line radiation is denoted as P_P. A typical plot of P_P/P_S as a function of discharge current I_d at constant pressure and frequency is shown in Fig. XV-15. The value of the discharge current at which the largest amplitude occurs

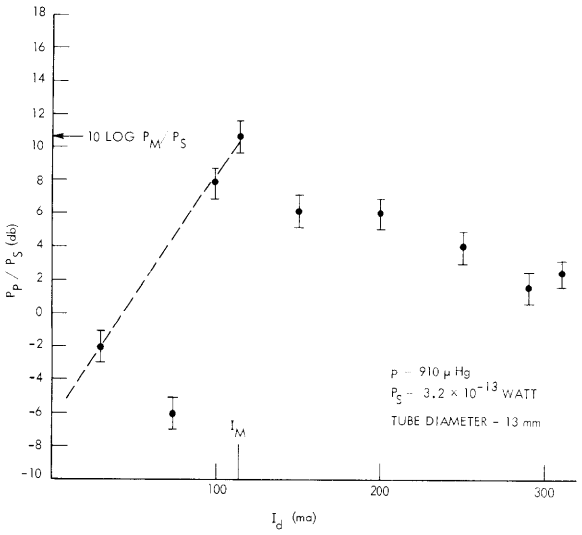

Fig. XV-15.

Radiometer measurements of amplitude of anomalous cyclotron radiation of a xenon plasma as a function of discharge current at constant pressure and microwave frequency.

is denoted I_M and the largest amplitude is denoted P_M.

If the collision frequency is assumed to have the form

$$\nu = a\, p\, v^{h-1},$$

where a and h are constants and v is the electron velocity, then the intensity of radiation from a tenuous plasma containing monoenergetic electrons[1] is

$$I_\omega = \frac{3}{3-h}\left[1 - \exp\left(-\frac{3-h}{3}\frac{\omega_p^2 L}{c\nu_o}\right)\right] B_\omega, \qquad (1)$$

where $\omega = \omega_b$ (ω_b is the electron-cyclotron frequency), and B_ω is the black-body intensity at a temperature equal to the average energy of the plasma electrons.

With h = 4.05 for xenon and L = 1 cm, the value of the exponent in Eq. 1 is positive and greater than unity for most values of electron density, temperature, and collision

frequency occurring in these experiments. With the value p = 900 μ Hg in Fig. XV-15, Eq. 1 can be approximated by

$$10 \log \frac{P_P}{P_S} = C + 3.035 \times 10^{-10} \frac{m}{P_c \sqrt{V}}. \tag{2}$$

Here, M is the electron density (electrons/cm^3), P_c is the collision probability, and

$$C = 10 \log 2.857 \frac{T_e}{T_S}, \tag{3}$$

where T_e is the electron temperature and T_S is the noise source temperature.

The dashed line in Fig. XV-15 in the range of discharge currents from 0 ma to 110 ma represent Eq. 2 when

$$\frac{m_o}{P_c \sqrt{V}} = 4.71 \times 10^{10}, \quad \frac{T_e}{T_S} = 1.5 \tag{4}$$

where m_o is the value of the electron density oocurring at I_d = 100 ma. If the value h = 4.46 supplied by Tanaka et al. is used,

$$\frac{m_o}{P_c \sqrt{V}} = 3.3 \times 10^{10}, \quad \frac{T_e}{T_S} = 1.1.$$

When the electron density is approximately 10^{11} cm^{-3} the plasma frequency is equal to the fixed frequency of the radiometer. The assumption of a reflectionless plasma employed in the derivation of Eq. 1 is not valid at this and higher densities. As the plasma becomes highly reflecting the emission should decrease. The amplitude of the narrow cyclotron line diminishes (Fig. XV-15) when the discharge current is increased beyond the value I_M = 110 ma. Several data points in Fig. XV-15 do not fall close to the dashed lines. Further experimental investigation is continuing to establish the P_P vs I_d curves for different pressures.

In Fig. XV-15 the value of the discharge current denoted I_M is believed to correspond to the condition $\omega_P = \omega$.

The electron density is a function of the ratio $I_d/(E/p)$. The discharge current required to maintain a fixed value of electron density decreases as the pressure increases. In Fig. XV-16 the discharge current required to hold the density at the constant value corresponding to $\omega_P = \omega$, that is, I_M, decreases with increasing pressure above 500 μ Hg. The behavior of I_M as a function of pressure below 500 μ Hg is not understood at present.

In Fig. XV-16 of Tanaka et al.[1] the value of I_M is 600 ma at a pressure of 260 μ Hg. This is approximately triple our value, as it should be, since their radiometer

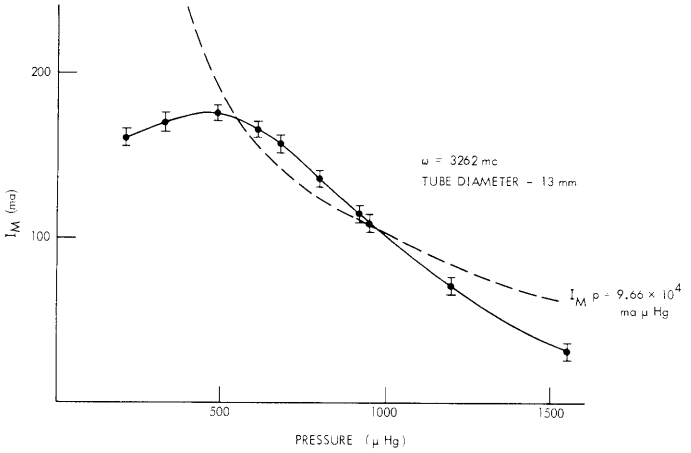

Fig. XV-16. Discharge current for a maximum radiated power as a function of xenon gas pressure.

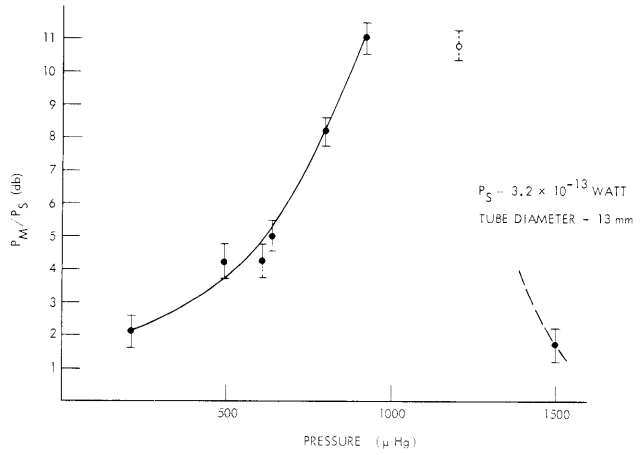

Fig. XV-17. Radiometer measurements of the maximum power radiated in the anomalous cyclotron radiation of a xenon plasma as a function of the gas pressure.

frequency is triple ours.

The value of P_P is a maximum at I_M, and is denoted P_M. P_M is plotted against pressure in Fig. XV-17. On the basis of Eq. 1 the amplitude of the narrow emission line should decrease with increasing pressure. Figure XV-17 shows the amplitude of P_M increasing with pressure in the range 200-1000 μ Hg. An uncertain experimental observation indicates that the value of P_M is fairly constant in the pressure range 1000-1200 μ Hg. Above 1200 μ Hg the value of P_M decreases rapidly with pressure. Several factors should be considered to obtain an adequate theoretical description of

Fig. XV-17. The electron temperature decreases with increasing gas pressure (cf. Brown[4]). Thus the number of electrons found at favorably low Ramsauer energies would increase with increasing pressure, thereby enhancing the emission. The rate of thermalization of the electron gas, however, also increases with pressure. Therefore, at higher pressure the amplitude of nonthermal radiation should decrease with increasing pressure.

Nonsynchronous observation of the output of the IF amplifier of the radiometer revealed that the narrow cyclotron line emission was pulsed rather than continuous. These pulses are so intense ($\sim 10^{-11}$-10^{-9} watt) that it is not necessary to use synchronous detection. The relative amplitude of these pulses as a function of magnetic field conform to the line shape shown in Fig. XV-14. That is, intense pulses occur only over a very narrow range of magnetic field.

A cw microwave signal was generated by a klystron mounted with several variable attenuators in a shielded box. The power output could be varied between 10^{-13} watt and 10^{-2} watt. The cw signal was modulated at 30 cps and transmitted through the plasma. The plasma emission was unmodulated.

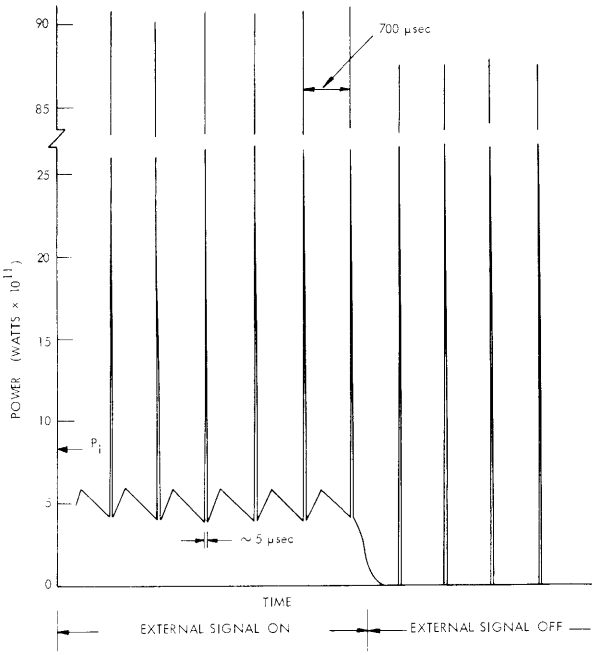

Fig. XV-18.

Power radiated by a xenon plasma at the cyclotron frequency as a function of time; power transmitted through the plasma from an external source. I_d = 25 ma; p = 500 μ Hg; $\omega = \omega_b$; IF bandwidth = 2 mc; P_i = incident power of external signal.

Figure XV-18 shows a period of time in which the klystron signal is incident on the plasma followed by a period in which the klystron signal is blocked off. The unmodulated plasma radiation is always present. The normal plasma radiation is too small, at this scale, to be seen, but the pulses are impressive. By careful adjustment of the discharge

current the pattern of pulses could be made stationary with respect to the modulating frequency and displayed on an oscilloscope. Figures XV-18, XV-19, and XV-20 are drawn from photographs of the oscilloscope patterns. The pulses occur at 700-μsec intervals when the discharge current is 25 ma and the gas pressure is 500 μ Hg. The width of the pulses was estimated to be less than 5 μsec. Variation between the amplitude of individual pulses was, at most, only a few per cent. No amplification of the transmitted part of the cw signal is evident. The detected power appears to be the sum of the plasma-attenuated cw signal plus the plasma generated pulses.

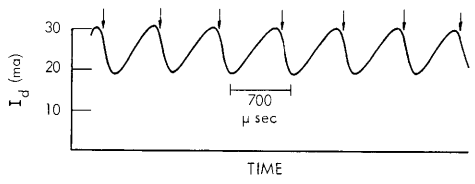

Fig. XV-19. Xenon plasma discharge current versus time. Arrows indicate time and current at occurrence of anomalous cyclotron radiation pulses.

Synchronous detection of the transmitted part of the modulated cw signal (with the plasma emission unmodulated) has not shown any tendency for the plasma to amplify external signals. Measurements were taken over the range from 10^{-13} watt to 10^{-2} watt.

Figure XV-18 further reveals that the transmitted cw signal is not constant in time. There is a saw-toothed oscillation with the same period as the plasma pulses. This variation in the absorption of the cw signal is due to a variation in the plasma density. Figure XV-19 shows the time variation of the discharge current. The arrows indicate the time and current values at which the plasma emits pulses. The discharge tube and a 100-ohm external resistor are in series with a constant voltage source. As the current (and density of electrons) increases, the voltage across the discharge decreases. $I_d R_{EXT} + V_d =$ constant. The electron temperature is probably a minimum when the pulses are emitted. A large inductance was placed in series with the discharge tube in order to maintain a constant discharge current. The pulses from the plasma persisted, but at random intervals.

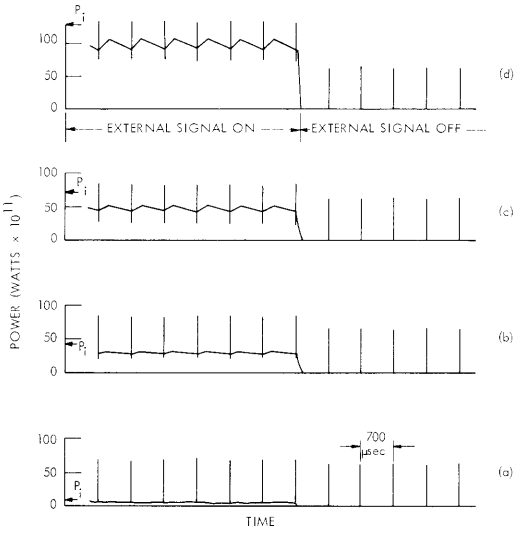

Fig. XV-20. Anomalous cyclotron pulses and transmitted portion of a P_i watt incident external signal.

Figure XV-20 shows the occurrence of absorption 'pulses' in the transmitted cw signal as the strength of the incident signal is increased. In the presence of

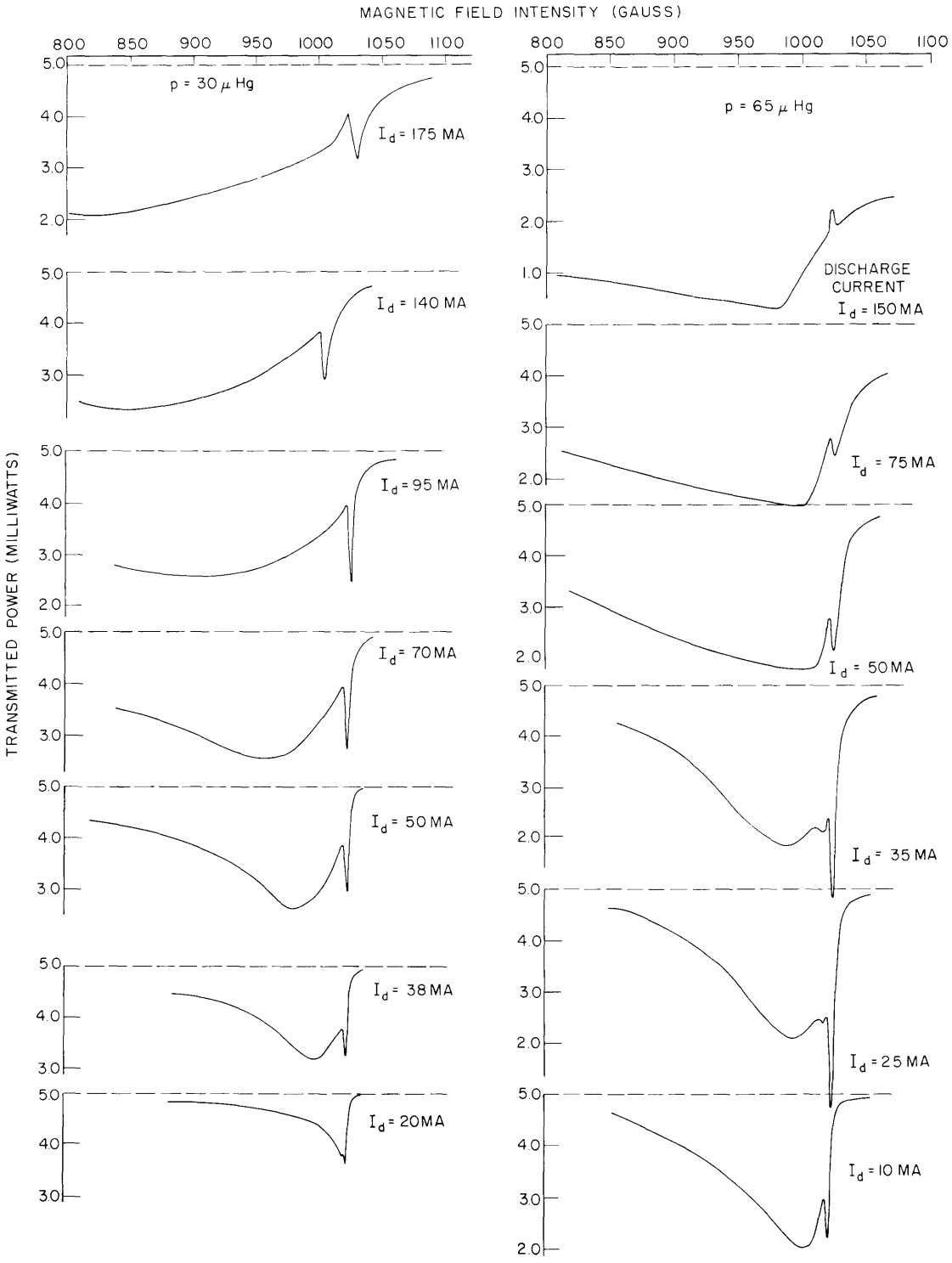

Fig. XV-21. Absorption of milliwatt microwave power by a xenon plasma as a function of magnetic field. Incident power = 5 mw.

an external signal the amplitude of the emitted pulse decreases while the amplitude of the absorption pulse increases with increasing signal. The time sequence of the two pulses has not been determined.

Figure XV-21 shows the power transmitted through the plasma as a function of magnetic field at milliwatt incident power. The narrow absorption line at the cyclotron frequency appears superimposed on a much broader 'normal' cyclotron absorption. The spectrum flattens out at higher discharge currents as the plasma approaches black-body conditions.

These experiments were repeated with helium. Helium does not contain a Ramsauer minimum in its electron collision cross section. The narrow-line cyclotron emission and absorption were not detected.

Many additional experiments are being undertaken. They will employ various gases, with and without Ramsauer minima. The radiation and absorption by these discharges will be measured in cavities, as well as in waveguides.

To summarize, intense pulses of radiation were observed in a xenon plasma. They occurred over a very narrow range of cyclotron frequencies centered at the fixed frequency of the detector. Synchronous detection of the transmitted portion of externally generated signals at levels comparable with the normal radiation from the plasma did not reveal amplification or additional absorption of the signal by the plasma. With the external signal comparable with the pulse height of the narrow-line emission, a narrow absorption line at the cyclotron frequency appears. This narrow absorption line is present when the external signal level is milliwatts.

No conclusive theoretical explanation for these phenomena are offered at this time. If the narrow-line radiation is due to amplification of the plasma radiation, the amplifier appears to be operating at saturation or poorly coupled to the external signal because no amplification of external signals has been detected. Another possibility is that there may occur a condition in which a large fraction of the electrons attain energies at the Ramsauer minimum. Since $P_c = 4$ at the minimum, they would radiate a very narrow line. The Ramsauer resonance is narrow and the electron lifetime at the minimum would be short. If the plasma were driven by a large external signal, this group of electrons would contribute to a narrow absorption line.

J. D. Coccoli

References

1. S. Tanaka, K. Mitani, and H. Kubo, Experiments on the Negative Radiation Temperature at Cyclotron Resonance in Cold Plasma, Research Report 1PPJ-6, Institute of Plasma Physics, Nagoya University, Japan, February 1963.

2. G. Bekefi, J. Hirshfield, and S. C. Brown, Phys. Fluids 4, 173 (1961); Phys. Rev. 122, 1037 (1961).

3. R. Q. Twiss, Australian J. Phys. 11, 564 (1958).

4. S. C. Brown, Basic Data of Plasma Physics (The Technology Press of the Massachusetts Institute of Technology, Cambridge, Mass., and John Wiley and Sons, Inc., New York, 1959); Special Technical Report No. 2, Research Laboratory of Electronics, M.I.T., August 17, 1959.